

Old Dominion University ODU Digital Commons

Electrical & Computer Engineering Faculty
Publications

Electrical & Computer Engineering

6-2002

CuIn_{1-x}Al_xSe₂ Thin Films and Solar Cells

P. D. Paulson

M. W. Haimbodi


S. Marsillac

Old Dominion University, Smarsill@odu.edu

R. W. Birkmire

W. N. Shafarman

Follow this and additional works at: https://digitalcommons.odu.edu/ece_fac_pubs

 Part of the [Electronic Devices and Semiconductor Manufacturing Commons](#), [Engineering Physics Commons](#), and the [Power and Energy Commons](#)

Repository Citation

Paulson, P. D.; Haimbodi, M. W.; Marsillac, S.; Birkmire, R. W.; and Shafarman, W. N., "CuIn_{1-x}Al_xSe₂ Thin Films and Solar Cells" (2002). *Electrical & Computer Engineering Faculty Publications*. 25.
https://digitalcommons.odu.edu/ece_fac_pubs/25

Original Publication Citation

Paulson, P., Haimbodi, M., Marsillac, S., Birkmire, R., & Shafarman, W. (2002). CuIn_{1-x}Al_xSe₂ thin films and solar cells. *Journal of Applied Physics*, 91(12), 10153-10156. doi: 10.1063/1.1476966

This Article is brought to you for free and open access by the Electrical & Computer Engineering at ODU Digital Commons. It has been accepted for inclusion in Electrical & Computer Engineering Faculty Publications by an authorized administrator of ODU Digital Commons. For more information, please contact digitalcommons@odu.edu.

CuIn_{1-x}Al_xSe₂ thin films and solar cells

P. D. Paulson, M. W. Haimbodi, S. Marsillac, R. W. Birkmire, and W. N. Shafarman^{a)}
Institute of Energy Conversion, University of Delaware, Newark, Delaware 19716

(Received 16 October 2001; accepted for publication 15 March 2002)

CuIn_{1-x}Al_xSe₂ thin films are investigated for their application as the absorber layer material for high efficiency solar cells. Single-phase CuIn_{1-x}Al_xSe₂ films were deposited by four source elemental evaporation with a composition range of 0 ≤ x ≤ 0.6. All these films demonstrate a normalized subband gap transmission >85% with 2 μm film thickness. Band gaps obtained from spectroscopic ellipsometry show an increase with the Al content in the CuIn_{1-x}Al_xSe₂ film with a bowing parameter of 0.62. The structural properties investigated using x-ray diffraction measurements show a decrease in lattice spacing as the Al content increases. Devices with efficiencies greater than 10% are fabricated on CuIn_{1-x}Al_xSe₂ material over a wide range of Al composition. The best device demonstrated 11% efficiency, and the open circuit voltage increases to 0.73 V. © 2002 American Institute of Physics. [DOI: 10.1063/1.1476966]

I. INTRODUCTION

Solar cells based on CuInSe₂ thin films have emerged as a leading candidate for low cost solar electric power generation. The CuInSe₂ band gap (E_g) can be increased to match the solar spectrum for higher efficiency by alloying the group III or VI elements. An increase in E_g of the absorber layer results in a tradeoff of higher open circuit voltage (V_{oc}) and lower short circuit current (J_{sc}) for the solar cell. The resulting decrease in series resistance loss may be advantageous for manufacture of photovoltaic modules by allowing use of a thinner transparent conducting oxide, typically ZnO, to reduce the optical losses. Alternatively, higher voltage and lower current can enable greater cell widths in module fabrication and smaller losses associated with cell interconnects. Also, a wider band gap should reduce the temperature coefficient of the solar cell performance to give increased output at typical operating temperatures, which may be as high as 60 °C. Finally, a wider band gap may enable CuInSe₂ based solar cells to be used as the top cell in a tandem or multi-junction cell configuration.

Significant work has been reported on the effect of the increased band gap by Ga addition on CuIn_{1-x}Ga_xSe₂ films and devices. The band gap of CuIn_{1-x}Ga_xSe₂ can be varied from 1.0 to 1.7 eV by changing the Ga/(Ga+In) ratio from 0 to 1. The efficiencies were found roughly independent of band gap for $E_g < 1.3$ eV.¹ The decrease in device efficiency with a greater band gap was attributed to a voltage dependent current collection¹ or to an increased defect density leading to greater recombination.²

CuIn_{1-x}Al_xSe₂ has been considered as an alternative to wider band gap CuIn_{1-x}Ga_xSe₂ based solar cells because it requires smaller relative alloy concentration than the Ga alloys to achieve a comparable band gap.³ Figure 1 shows the variation in the lattice constant with the band gap when alloying CuInSe₂ with Ga or Al.^{4,5} The change in the lattice constant with alloying is smaller for Al than Ga for a film

with a similar band gap. This means that alloying with Al may help to achieve a higher band gap with less change in the structural properties of CuInSe₂.

Previous work reported in the literature on CuIn_{1-x}Al_xSe₂ alloys has focused primarily on single crystal⁶ or polycrystal ingots.^{7,8} Characterization of these crystals includes optical spectroscopy and phase and structural analysis by x-ray diffraction (XRD). Thin films of CuIn_{1-x}Al_xSe₂ deposited by the reaction of stacked layers were reported and also characterized by XRD and optical spectroscopy.⁹ This article describes the deposition and characterization of single phase CuIn_{1-x}Al_xSe₂ thin films with a varying band gap deposited by multisource elemental evaporation and the fabrication of CuIn_{1-x}Al_xSe₂ based solar cells.

II. EXPERIMENTAL PROCEDURE

Polycrystalline CuIn_{1-x}Al_xSe₂ films were deposited by four-source evaporation of elemental Cu, In, Al, and Se using Knudsen type sources in which the elemental fluxes were coincident onto soda lime glass or Mo-coated soda lime glass substrates. A base pressure of 4×10^{-6} Torr was attained prior to the CuIn_{1-x}Al_xSe₂ deposition. Elemental fluxes

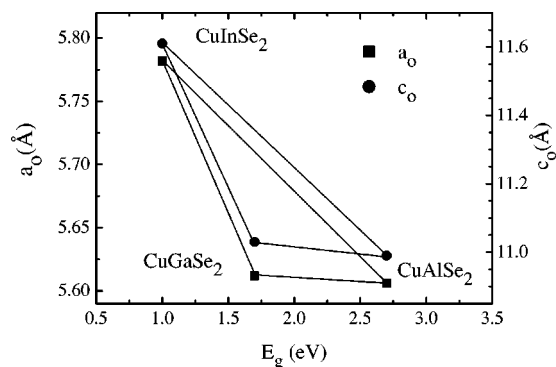


FIG. 1. Variation in the lattice constants a_0 and c_0 with a band gap for CuInSe₂ alloys with Ga or Al.

^{a)}Electronic mail: wns@udel.edu

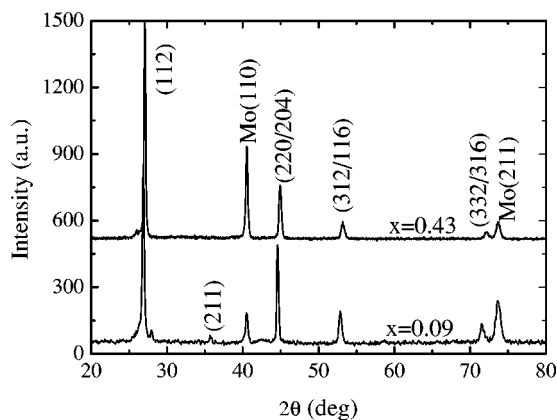
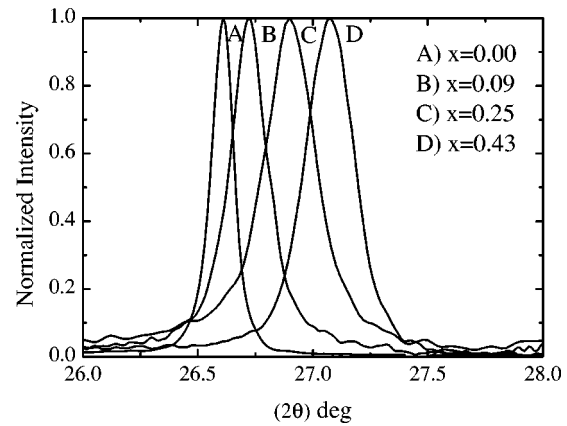
TABLE I. Composition of $\text{CuIn}_{1-x}\text{Al}_x\text{Se}_2$ films measured by EDS.

Cu(%)	In(%)	Al(%)	Se(%)	Al/(Al+In)
CuIn _{1-x} Al _x Se ₂ films used for optical measurements				
22.2	25.2	0.0	52.6	0.00
21.0	25.9	2.4	50.7	0.08
20.4	23.2	5.5	50.9	0.19
21.3	19.4	8.9	50.4	0.31
20.4	16.9	13.0	49.7	0.43
19.8	12.1	17.2	50.9	0.59
CuIn _{1-x} Al _x Se ₂ films used for XRD measurement and device fabrication				
22.4	27.1	0.0	50.5	0.00
20.8	25.3	2.4	51.5	0.09
21.2	21.7	7.4	49.8	0.25
21.0	17.0	12.6	49.4	0.43

were independently controlled by controlling the source temperatures. Constant elemental fluxes were used throughout the deposition of the $\text{CuIn}_{1-x}\text{Al}_x\text{Se}_2$ films so that there was no intentional grading of the composition through the films. A typical 1 h deposition resulted in 2- μm -thick $\text{CuIn}_{1-x}\text{Al}_x\text{Se}_2$ films. The films were deposited at a substrate temperature of 450 °C since films deposited at higher temperatures frequently did not adhere well and flaked off at the $\text{CuIn}_{1-x}\text{Al}_x\text{Se}_2/\text{Mo}$ or $\text{CuIn}_{1-x}\text{Al}_x\text{Se}_2/\text{glass}$ interface.

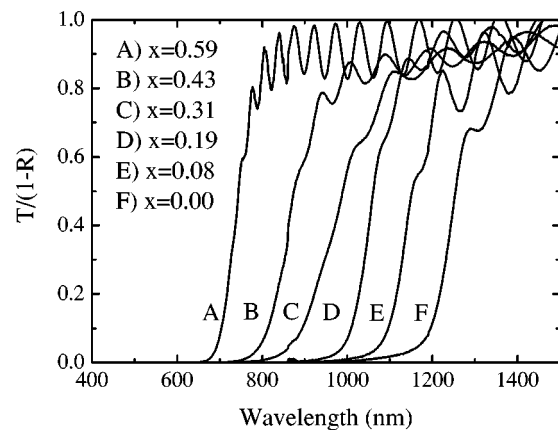
The composition of the $\text{CuIn}_{1-x}\text{Al}_x\text{Se}_2$ films were measured by energy dispersive x-ray spectroscopy (EDS) in an AMRAY 1810 scanning electron microscope attached with an Oxford Instruments Energy200 EDS analytical system at 22.5 kV accelerating voltage. Wavelength dispersive spectroscopy (WDS) measurements, which give better resolution of the Al and Se peaks than the EDS spectra, were used to calibrate and provide standards for the EDS measurements. XRD patterns of the $\text{CuIn}_{1-x}\text{Al}_x\text{Se}_2$ films were obtained using a Philips/Norelco diffractometer with Bragg-Bretano (θ - 2θ configuration) focusing geometry and Cu $K\alpha$ radiation. 2θ scans taken at 0.03° step size were used to identify the phases present in the films.

Optical transmission and reflection were measured on a Perkin-Elmer Lambda 9 Spectrophotometer equipped with an integrating sphere. Optical properties n and k were obtained using a J. A. Woollam rotating analyzer variable angle

FIG. 2. XRD spectra for two $\text{CuIn}_{1-x}\text{Al}_x\text{Se}_2$ films with $x=0.09$ and 0.43 .FIG. 3. XRD spectra showing the shift in (112) peak position with x .

spectroscopic ellipsometer (VASE) with an autoretarder.¹⁰ $\text{CuIn}_{1-x}\text{Al}_x\text{Se}_2$ films are washed in de-ionized water prior to the ellipsometric measurement to remove water-soluble sodium compounds from the film surface. The $\text{CuIn}_{1-x}\text{Al}_x\text{Se}_2$ films are relatively smooth, compared to typical $\text{CuIn}_{1-x}\text{Ga}_x\text{Se}_2$ films, with rms roughness measured by atomic force microscopy less than 30 nm. This enables the VASE analysis to determine the optical properties unambiguously. Since no literature data were available for optical constants of thin film $\text{CuIn}_{1-x}\text{Al}_x\text{Se}_2$, a parametric dispersion model was developed to fit the optical data. A detailed description of the optical model and fit used in this analysis is beyond the scope of this article and will be published separately.

Solar cells were fabricated by chemical bath deposition of CdS. The base line processes originally developed for $\text{Cu}(\text{InGa})\text{Se}_2$ devices have been reported elsewhere.¹ Completed devices have the structure glass/Mo/ $\text{CuIn}_{1-x}\text{Al}_x\text{Se}_2$ /CdS/ZnO:Al/Ni-Al grid, with total cell area of 0.47 cm^2 defined by mechanical scribing. The devices were characterized by J - V measurements under 100 mW/cm^2 AM 1.5 illumination at 25 °C and by quantum efficiency (QE) measurement under white light bias.

FIG. 4. $T/(1-R)$ for $\text{CuIn}_{1-x}\text{Al}_x\text{Se}_2$ films with varying x .

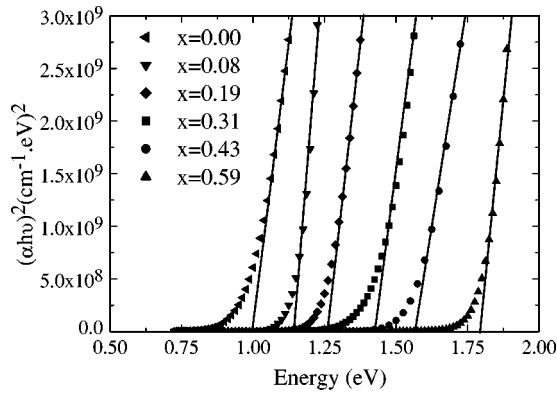


FIG. 5. $(ahv)^2$ vs hv plots for $\text{CuIn}_{1-x}\text{Al}_x\text{Se}_2$ with varying Al content.

III. RESULTS

A. Structural and optical characterization

Table I shows the composition of $\text{CuIn}_{1-x}\text{Al}_x\text{Se}_2$ films characterized in this article, as determined by the EDS measurements. The top section of the table lists samples deposited on bare glass for optical characterization and the bottom section samples deposited on Mo-coated glass used for other characterization and device fabrication. For all films, the oxygen concentration is below the EDS detection limit $\sim 0.5\%$. With $x > 0.6$, $\text{CuIn}_{1-x}\text{Al}_x\text{Se}_2$ films were previously shown to contain oxygen,³ which may have resulted from the reaction with air after deposition, rather than oxygen incorporation during deposition.

The $\text{CuIn}_{1-x}\text{Al}_x\text{Se}_2$ films are all found to be single phase within the detection limits of XRD analysis. XRD spectra for two films with $x = 0.09$ and 0.43 are shown in Fig. 2. All peaks shown correspond to either $\text{CuIn}_{1-x}\text{Al}_x\text{Se}_2$ or Mo. As the Al content increases, the position of the $\text{CuIn}_{1-x}\text{Al}_x\text{Se}_2$ peaks shift to higher 2θ due to a decrease in lattice spacing. This is clearly seen by the normalized (112) reflections shown for four films in Fig. 3.

The normalized optical transmission, $T/(1-R)$, for five $\text{CuIn}_{1-x}\text{Al}_x\text{Se}_2$ films and a CuInSe_2 film is shown in Fig. 4. All films show a subband gap transmission $T/(1-R) > 0.85$. This is one of the criteria for a wide band gap material to be

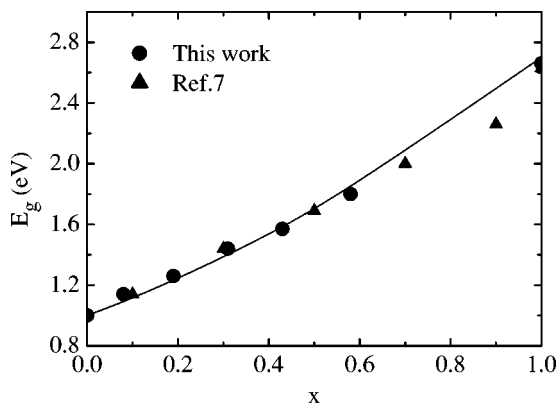


FIG. 6. Variation in the $\text{CuIn}_{1-x}\text{Al}_x\text{Se}_2$ band gap with Al content. The line is a fit of the data in this work to the Eq. (1) with $b = 0.62$.

TABLE II. $J-V$ parameters for the best cells with different Al concentrations and band gaps obtained from EDS and QE measurements.

x	V_{oc} (V)	J_{sc} (mA/cm^2)	FF (%)	Eff. (%)	E_g (EDS) (eV)	E_g (QE) (eV)
0.00	0.422	34.4	68.7	10.0	1.00	1.00
0.09	0.517	30.6	69.7	11.0	1.10	1.10
0.25	0.630	25.5	65.8	10.6	1.32	1.25
0.43	0.731	22.0	67.1	10.8	1.57	1.52

used in the top cell of a tandem solar cell configuration. The band edge is shifted towards higher energies as the Al concentration increases.

VASE was used to determine the absorption coefficient, α , and Fig. 5 shows the plot $(ahv)^2$ vs hv for $\text{CuIn}_{1-x}\text{Al}_x\text{Se}_2$ films with varying x , which was used to determine E_g from extrapolation of the linear portion of each curve. The band gap of $\text{CuIn}_{1-x}\text{Al}_x\text{Se}_2$ with $x = 0$ agrees with the value reported in the literature on CuInSe_2 ¹¹ verifying the validity of this analysis. The band gap increases with increasing Al content as shown in Fig. 6. Also shown is the band gap variation reported by Gebicki *et al.*⁷ measured on $\text{CuIn}_{1-x}\text{Al}_x\text{Se}_2$ polycrystalline ingots. The compositional dependence of the band gap can be fit to

$$E_g(x) = (1-x)E_g(A) + xE_g(B) - bx(1-x), \quad (1)$$

where $E_g(A) = 1.0$ eV is the band gap of CuInSe_2 , $E_g(B) = 2.7$ eV is the band gap of CuAlSe_2 , and b is the optical bowing parameter. The least squares fit shown in Fig. 6 gives $b = 0.62$. The bowing parameter obtained in this work is larger than the value 0.51 reported by Gebicki *et al.*⁷ and comparable to the value 0.59 calculated by Wei and Zunger.⁴

B. Device results

The $J-V$ parameters for the best cells with E_g ranging from 1.00 to 1.57 eV are listed in Table II. Figure 7 shows the $J-V$ curves for these devices measured under illumination and in the dark. V_{oc} increases monotonically with increasing Al content. The best device has 11% efficiency and there is no decrease in efficiency as E_g increases up to 1.57 eV.

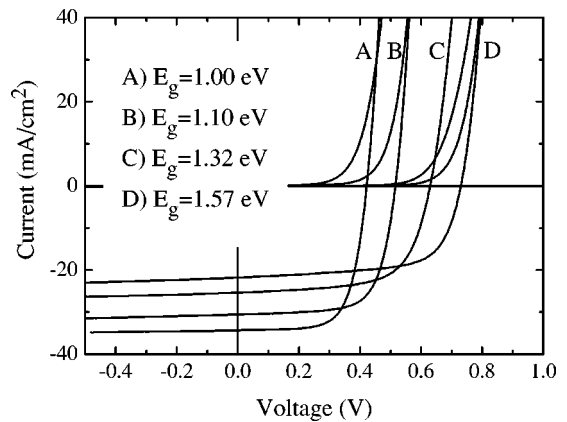


FIG. 7. $J-V$ curves in the dark and under illumination for $\text{CuIn}_{1-x}\text{Al}_x\text{Se}_2$ devices with a varying band gap.

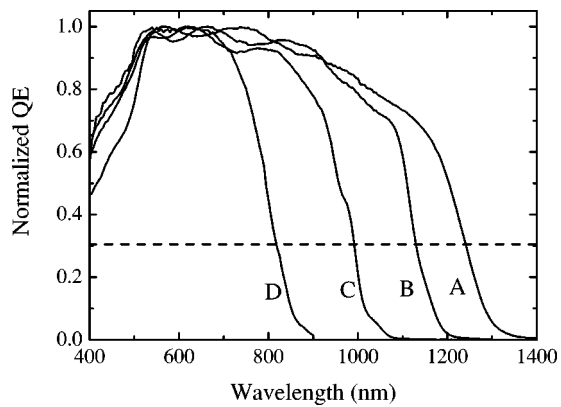


FIG. 8. Quantum efficiency for the $\text{CuIn}_{1-x}\text{Al}_x\text{Se}_2$ devices identified in Fig. 7.

Quantum efficiency curves for these devices are shown in Fig. 8. The long wavelength edges of the curves shift to higher energy with an increasing Al content and are consistent with the band gaps obtained from the compositions and optical measurements. A straight line parallel to the x axis was drawn in Fig. 8, intercepting curve A ($x=0$) at 1240 nm ($E_g=1.00$ eV). The intercepts of this line with the other QE curves give the apparent band gaps for different Al content. Table II also shows the comparison of the band gaps obtained from composition using Eq. (1) with $b=0.62$ and apparent band gaps obtained from QE.

$\text{CuIn}_{1-x}\text{Ga}_x\text{Se}_2$ solar cells have been reported to show an improvement by air annealing, typically at 200°C .¹² Similar enhancement in the device performance was investigated in the $\text{CuIn}_{1-x}\text{Al}_x\text{Se}_2$ devices. Typically, V_{oc} increased by 20–60 mV after air annealing for 3 min at 200°C of $\text{CuIn}_{1-x}\text{Al}_x\text{Se}_2$ devices with $x>0.1$. With lower Al content, there was no improvement in V_{oc} . In general, the increase in the V_{oc} is accompanied by a decrease in the fill factor (FF) and J_{sc} and, hence, the device efficiency decreases. However, some of the higher Al devices show an increase in V_{oc} , J_{sc} , and FF with air annealing. The mechanism that distinguished this device behavior is not understood.

IV. CONCLUSIONS

The deposition of single phase $\text{CuIn}_{1-x}\text{Al}_x\text{Se}_2$ thin films with band gap from $1.00\text{ eV} \leq E_g \leq 1.57\text{ eV}$ has been demonstrated. The optical band gap was determined from ellipsometry measurements and gave a bowing parameter $b=0.62$. Devices were fabricated over a wide range of composition with efficiencies of 10% to 11%. V_{oc} has been increased from 422 to 731 mV with no decrease in efficiency. However, V_{oc} and efficiency are smaller than $\text{CuIn}_{1-x}\text{Ga}_x\text{Se}_2$ cells with a comparable band gap.¹

ACKNOWLEDGMENTS

The authors thank J. Titus, K. Hart, T. Hughes-Lampros, and R. Dozier for technical assistance and Sally Asher and Matt Young at the National Renewable Energy Laboratory for WDS measurements. This work was supported, in part, by NIST under an Advanced Technology Program in collaboration with ITN Energy Systems and Global Solar Energy.

- ¹W. N. Shafarman, R. Klenk, and B. E. McCandless, *J. Appl. Phys.* **79**, 7324 (1996).
- ²U. Rau, M. Schmidt, A. Jasenek, G. Hanna, and H. W. Schock, *Sol. Energy Mater. Sol. Cells* **67**, 137 (2001).
- ³M. W. Haimbodi, E. Gourmelon, P. D. Paulson, R. W. Birkmire, and W. N. Shafarman, *Proc. 28th IEEE Photovoltaic Specialists Conference*, Anchorage, Alaska, 2000, p. 454.
- ⁴S. Wei and A. Zunger, *J. Appl. Phys.* **78**, 3846 (1995).
- ⁵International Center for Diffraction Data, ICDD PDF-2 database, 1996.
- ⁶I. V. Bodnar and I. N. Tsyrelchuk, *J. Mater. Sci. Lett.* **13**, 762 (1994).
- ⁷W. Gebicki, M. Igalson, W. Zajac, and R. Trykozko, *J. Phys. D* **23**, 964 (1990).
- ⁸C. A. Durante Rincón, M. T. Mora, and M. León, *Inst. Phys. Conf. Ser.* **152**, 123 (1998).
- ⁹F. Itoh, O. Saitoh, M. Kita, H. Nagamore, and H. Oike, *Sol. Energy Mater. Sol. Cells* **50**, 119 (1998).
- ¹⁰J. A. Wollam, B. Johs, C. M. Herzinger, J. N. Hilfiker, R. Synowicki, and C. Bungay, *Proc. SPIE* **CR72**, 3 (1999).
- ¹¹H. Neumann *Sol. Cells* **16**, 399 (1986).
- ¹²D. Cahen and R. Noufi, *Appl. Phys. Lett.* **54**, 558 (1989).

Journal of Applied Physics is copyrighted by the American Institute of Physics (AIP). Redistribution of journal material is subject to the AIP online journal license and/or AIP copyright. For more information, see <http://ojps.aip.org/japo/japcr/jsp>
Copyright of Journal of Applied Physics is the property of American Institute of Physics and its content may not be copied or emailed to multiple sites or posted to a listserv without the copyright holder's express written permission. However, users may print, download, or email articles for individual use.